Temporal variability of the snow meteorological parameters over Antarctic continental icesheet and estimation of surface energy budget in Dronning Maud Land, East Antarctica

Prabhat Sahoo and Ashwani Acharya

Snow & Avalanche Study Establishment, Chandigarh, India-160036
E-mail: prabhat4u2@gmail.com

Abstract

Meteorological parameters were observed over continental icesheet in Dronning MaudLand, East Antarctica ear Indian Research Station Maitri for a period of 13months from 1 November 2010 to 30 November 2011 using an Automatic Weather Station. It is located at S70°47'40.9", E11°41'43.1" at an altitude of 395ma.s.l, and measures air temperature, relative humidity, wind speed, and direction, incoming and reflected solar radiation, pressure, and snow temperature. Cloud measurements were done by visual inspection, a simple model was used to evaluate the Surface-energy balance from measured meteorological quantities. Large temporal variability is observed in different estimated energy fluxes throughout the year. Observed low relative humidity (yearly average 57%) and high katabatic winds (yearly average of 10.7 m/sec) lead to a high ablation rate (main sublimation in winter and melting, evaporation/ sublimation in summer) of the glacier ice at the observation ocation. Constant cooling of the icesheet by emission of longwave radiation observed throughout the study period. Effective short wave flux and sensible heat flux were observed as the main heat source for the glacier. It is observed that the Antarctic icesheet is continuously ablating high energy compared to its accumulation, in the form of longwave radiation and turbulent flux of latent heat, which leads to a negative energy balance of the icesheet throughout the year,even during the Antarctic summer period.

Keywords: Surface energy balance, Antarctica, shortwave flux, longwave flux, latent heat, sensible heat

1. INTRODUCTION

Snow and Avalanche Study Establishment, Manali, India has taken up along term project of the study of Surface Energy Balance of the continental icesheet in Dronning Maud Land area, Antarctica. The project work started since 25th Indian Scientific Expedition to Antarctica (25th ISEA) in December 2005. In the present paper the results are presented based on the data observed during 30th ISEA.

Glacier gains and loses energy by various processes. It gains heat from insolation, longwave radiation from atmosphere and clouds, advection of warm air, latent heat released by condensation of moisture on the glacier surface, sensible heat transfer if air is warmer than glacier surface and conduction from ground underneath. On the other hand glacier loses heat to its environment by longwave radiation, evaporation or sublimation from glacier surface and sensible heat if air is colder than the surface of the glacier1. The net energy gained is used in raising the temperature of the glacier and melting of ice. Hence the energy balance approach can be used to determine the ablation processes at the surface of the glacier and quantification of the physical processes can be helpful to understand the health of the glacier. Various glacier mass balance models have been developed based on calculation of all energy transfers between the atmosphere and the glacier surface 2-4. The energy balance model is an attractive tool for simulating the surface balance, since the physical processes on the surface can be described fairly explicitly in the model 5.The surface- energy balance over Antarctic snow/ ice surfaces has been extensively studied by Bintanja et. al 1994, Braun et. al 2000, Van Den Broeke et. al., 2006, VanDen Broeke et.al.2005, Mishra,1999. But most of the studies have been restricted to two-three months of the summer season of the continent. In the present paper the surface energy balance for one complete year including summer and winter period of the continent is presented.

2. OBSERVATION SITE AND DATA OBSERVATIONS

Indian Research Station "Maitri" islocated in 'Schirmacher Oasis' in the coastal margin of the Dronning Maud Land, East Antarctica at S70°45.94 'and E11°44.13'. Automatic Weather Station (make Campbell scientific) was installed over continental icesheet of Antarctica at S 70°47'40.9", E 11°41'43.1" at a distance of around 5Km from Indian station at an elevation of 395m from mean sea level and the Observation site is shown by figure 1.The Antarctic environment shows a number of challenges to those involved in making meteorological Observations. Extreme cold, strong winds, icing and blowing snow all adversely affect instruments, making the observer's task a difficult one10. The AWS was installed on 24Feb2006 during Antarctic summer period and consists the following calibrated sensors.

a. Wind Direction and Wind Speed sensor (Propeller Vane type) of make RMYOUNG for measuring wind speed and direction. Sensor is capable of measuring wind speed in the range of 0 - 50ms-1 with an accuracy of $\pm$0.3ms-1 and gust survival of 60ms-1 . Sensor can measure wind direction with accuracy of $\pm$3degrees and range 360degrees.

b. AT/ Rh sensor to measure air temperature and relative humidity. It measures air temperature in the range of +50°C to-50°C with an accuracy of $\pm$0.3°C and relative humidity with an accuracy of $\pm$3% from 0% to 90% and $\pm$4% from 90% to100%.

c. Pressure transducer located in the enclosure can measure atmospheric pressure from 400mb to 1100mb with an accuracy of 0.5mb.

d. Upward and downward looking pyranometers of make Kipp and Zonen measures incoming and outgoing radiation and measures shortwave radiation in the wavelength range of 305-2800nm with cosine error of $\pm$1% from 0 to 70°zenith and $\pm$3% from 70° to 80°zenith angle.

e. IR-based snow surface temperature sensor measures snow surface temperature in the range of +50°C to -50°C with an accuracy of $\pm$0.3°C.

The whole system is powered by 100 Ampere-Hour battery located inside the enclosure mounted near the base of the tower. The battery is recharged during periods of sunlight by a solar panel fixed near the top of the tower. During the Antarctic summer period the battery is fully charged due to prolong sunshine hours and keeps the system functional during long periods of polar nights. The AWS records the hourly observations of air temperatures (Maximum temperature, Minimum temperature, Instantaneous temperature and hourly average temperature), snow surface temperature, relative humidity, wind speed and direction, incoming solar radiation, reflected solar radiation and atmospheric pressure. These observations are continuously stored in the data logger CR23X, located inside the enclosure. The data can be downloaded from the AWS with the help of downloading storage module. The AWS was visited periodically for manual downloading of the data from the data logger (as data reception facility through satellite was not available at Indian Research Station) and maintenance work to minimise the data losses. Apart from the AWS data, cloud observations for cloud type and cloud amount have been observed manually from conventional surface observations.

3. ENERGY BALANCE MODEL

The principal fluxes of energy at the Earth's surface are the net radiative flux and the atmospheric fluxes of sensible heat and latent heat. The net energy exchange between the earth and the atmosphere is the residual of these energy fluxes10. Net change in energy storage of a glacier ΔQ is expressed as:

$$\Delta Q = SHW\downarrow + SHW\uparrow + LW\downarrow + LW\uparrow + SHF + LHF + G \quad (1)$$

$$= SHWnet + LWnet + SHF + LHF + G \quad (2)$$

$$= Rnet + SHF + LHF + G \quad (3)$$

Where SHW$\downarrow$-Incomingshortwaveradiation flux SHW$\uparrow$ -Reflected short wave radiation flux LW$\downarrow$-Incoming Long wave radiation flux L W$\uparrow$ - Emitted Long wave radiation flux

SHF -Sensible heat flux

LHF -Latent heat flux

G -Sub surface conductive heat flux

All terms are estimated at the surface and are defined positive when directed towards the surface. Contribution of the subsurface conductive heat flux to the net energy exchange at the glacier surface is very little compared to other fluxes, so the net change in energy storage of the glacier is expressed by the following equation in the model.

$\Delta Q = Rnet + SHF + LHF$(4)

Short-Wave Radiation Flux

Short-wave or solar radiation drives the general circulation of the atmosphere and the weather systems that are observed on a day-to-day basis10. Most of this energy is absorbed in the tropics and mid-latitude areas, with the Polar Regions receiving much less as a result of the low angle of the sun at these latitudes. The high albedo (reflectivity) of the snow and ice surface also results in much of the incoming solar radiation being returned to spaces to that the fraction absorbed is much less than that is absorbed in the extra Polar Regions. Even after higher surface reflectivity, radiation is extremely important in determining the surface energy budget of the Antarctica, as it affects many aspects of the Antarctic climate. Downwelling or global solar radiation (SHW$\downarrow$) consists of two components: a direct element which arrives from the solid angle subtended by the sun's disk and a diffuse component, which arrives from the remainder of the sky. The reflected solar radiation (SHW$\uparrow$) is the upwards shortwave radiation that has been reflected by the surface and diffused by atmospheric particles in the layer between the surface and the observation point. When the reflected solar radiation measured close to ground the diffused partis very small. The ratio of the reflected shortwave radiation to the global solar radiation is called the albedo(α) of the surface and is important in determining what proportion of downwelling solar radiation is absorbed at the surface. The albedo of the glacier surface varies considerably across the Antarctic and according to season. The amount of solar radiation absorbed by The surface is called the net short-wave radiation (SHWnet) and is defined as the global radiation less the reflected shortwave radiation. The expression for the net shortwave radiation can be written as:

$$SWnet = SHW\downarrow - SHW\uparrow = SHW\downarrow(1-\alpha) \quad (5)$$

3.1 Long Wave Radiation Flux

The exchange of longwave radiation in the wavelength range 3 μm–40 μm is confined to the snow/ice surface only. The net longwave radiation (LWnet) at the glacier surface is the sum of the upward terrestrial component LW↑ (negative) and the downward LW↓ (positive) radiation emitted by the clouds and gases.

The upward component is usually greater than the downwelling flux, so net longwave flux is generally negative and expresses the loss of energy from the glacier surface in the longwave part of the electromagnetic spectrum. The downwelling longwave radiation component (LW↓) is dependent on the vertical distribution of temperature and water in the atmosphere and the optical properties of any clouds present.

In the absence of clouds, LW↓ is dominated by emission from atmospheric water vapor and carbon dioxide. Even in the relatively dry Antarctic atmosphere, there is sufficient water vapor for the dominant contribution to LW↓ to come from atmospheric emission at relatively low levels. Under conditions of total low cloud cover, LW↓ will be dominated by emission from cloud water droplets and ice particles.

As downwelling longwave radiation depends on the temperature and composition of the atmosphere, this is estimated using a model developed by Prata (1996). The model computes the emissivity of the atmosphere (em) depending on precipitable water content.

The model works well in the limit of a dry atmosphere:

$$LW\downarrow = \epsilon m \sigma Ta^4 \quad (6)$$

Where, $\epsilon m = 1 - (1 + w)\exp\{-(1.2 + 3.0w)^{1/2}\}$ *(7) and*

$$w = 46.5(ea/Ta) \quad (8)$$

Here, ***ea*** *is the vapor pressure (Pa) and* **Ta** *is the absolute temperature measured at 1.5–2.0 m height above the surface.*

LW↑ is the emitted terrestrial longwave radiation and can be computed from the Stefan-Boltzmann Law, as the snow/ice surface is assumed to be a nearly perfect blackbody in the longwave portion of the electromagnetic spectrum. Experimentally determined emissivities for snow surfaces were found to be in general agreement with modeled values estimated by Dozier and Warren (1982), and these values were close to one. Emitted Longwave Radiation can be computed as:

$$LW\uparrow = \epsilon s \sigma Ts^4 \quad (9)$$

Where,

σ is the Stefan-Boltzmann constant (5.67 x 10^{-8} $Wm^{-2}K^{-4}$), Ts is the radiative temperature of the surface in kelvins, and ϵs *is the surface emissivity.*

On a cloud-free day, the net Longwave Radiation absorbed by the glacier surface is:

$$LWnet = LW\downarrow - LW\uparrow \quad (10)$$

$$= \epsilon m \sigma Ta^4 - \epsilon s \sigma Ts^4 \quad (11)$$

Clouds significantly affect net Longwave Radiation. In general, downwelling Longwave Radiation in the presence of clouds may be assumed as the blackbody radiation emitted at the cloud base temperature (Tc). As clouds, being composed of liquid water droplets, absorb much more LW radiation than water vapor, they act as nearly perfect blackbodies.

Under overcast sky conditions, the net Longwave Radiation is given by:

$$LWnet = \epsilon m \sigma Tc^4 - \epsilon s \sigma Ts^4 \quad (12)$$

he main role of cloudiness is to reduce the loss of LW radiation. If **N** is the amount of cloudiness in terms of the fraction of the sky covered, then:

$$LWnet = \{\epsilon m \sigma Ta^4 - \epsilon s \sigma Ts^4\}(1 - kN) \quad (13)$$

Where **k** is a coefficient and depends on the type and height of clouds. Experimental values reported by the US Army Corps of Engineers (1956) are:

k = 0.76 for low and thick clouds

k = 0.52 for medium clouds

k = 0.26 for high clouds

3.2 Sensible Heat Flux

Sensible heating represents the combined processes of conduction and convection. Generally, the snow surface is colder than the air above it, and heat transfers from warm air to the colder snow surface through sensible heating, allowing the glacier surface to gain energy. In case of temperature inversion, heat transfer occurs in the opposite direction, causing the glacier surface to lose energy.

The vertical turbulent-sensible heat flux (SHF) is expressed in flux-gradient form as:

$$SHF = \rho CpKH(\delta T/\delta z - \Gamma) \quad (14)$$

Where:

- **ρ** is the density of air,
- **Cp** is the specific heat of air (1005 J kg^{-1} K^{-1}),
- **KH** is the coefficient of turbulent diffusivity,
- **$\delta T/\delta z$** is the vertical temperature gradient, and
- **Γ** is the adiabatic lapse rate.

In this study, air temperature observations are taken at a sensor height of 2 m above the glacier surface, dealing with an air layer close to the glacier surface. In this layer, air temperature gradients are large compared to the adiabatic lapse rate, so **Γ** is neglected compared to **$\delta T/\delta z$** in Equation (14).

Equation (14) can be reformulated in terms of simple data for wind speed and temperature as follows:

$SHF = (C_p\rho_0/P_0)K_nPu(T_a - T_s)$ (15)

Where:

- **$K_n = k^2 / [\log(z_a/z_0)]^2$** (16)

Where **ρ_0** is the density of air (1.29 kg m^{-3}) at the standard atmospheric pressure **P_0** (1.013 x 10^5 Pa), **Kn** is a dimensionless transfer coefficient, **P** is the mean atmospheric pressure at the measuring site, and **u** and **Ta** are the measured wind speed and air temperature at a height of 2 m above the glacier surface. **k** is von Karman's constant (0.41), **za** is the sensor height above the ground (2 m), and **z_0** is the aerodynamic roughness length, for which a value of 0.001 m is adopted for an ice surface.

3.3 Latent Heat Flux

Latent heat flux is an important component of the surface energy budget and is carried by turbulent transport in the atmospheric boundary layer. By analogy with the sensible heat flux, the latent heat flux is given by:

$LHF = L_v(0.623\rho_0/P_0)K_n\,u\,(e_a - e_s)$ (17)

Where **Lv** is the latent heat of vaporization, **ea** is the vapor pressure at height **z** above the glacier surface, and **es** is the saturation vapor pressure at the glacier surface. The latter is a function of the surface temperature and is 611 Pa for a melting surface. For distinguishing between sublimation and condensation, guidelines given by Ambach and Kirchlechner (1986) and Greuell and Konzelmann (1994) have been followed.

- For condensation: **$L_v = 2.514$ MJ kg^{-1}**
- For sublimation: **$L_v = 2.849$ MJ kg^{-1}**

When (ea - es) is positive and Ts = 0°C, water vapor condenses as liquid water on the melting glacier surface with Lv = 2.514 MJ kg^{-1}. When (ea - es) is negative, sublimation occurs with Lv = 2.849 MJ kg^{-1}. Also, when (ea - es) is positive and Ts < 0°C, deposition from vapor to solid ice occurs with Lv = 2.849 MJ kg^{-1}.

The equations for sensible and latent heat fluxes are applicable for neutral atmospheric conditions. In Antarctica, the atmospheric conditions above the ice sheet are rarely neutral, and the equations can be applied with stability corrections for the transfer coefficient Kn in terms of the Richardson number (Ri).

- For unstable conditions (Ri < 0):
  $Kw^2 = Kn(1 - 10Ri)$
- For Ri = 0:
  $Kw^2 = Kn$
- For stable conditions (Ri > 0):
  $Kw^2 = Kn / (1 + 10Ri)$

(Source: Price and Dunne, 1976).

4. RESULTS AND DISCUSSION

4.1 Variation of Meteorological Parameters

Figures 2(a), 2(b), 2(c), 2(d), 2(e), and 2(f) present the variation of daily averaged values of air temperature, wind speed, relative humidity, atmospheric pressure, total sunshine hours, and fraction of cloud cover at the AWS location during the observation year. From the hourly observations of these parameters, the daily averages have been calculated.

Daily average air temperature varies between -28.9°C (observed on 5-August-2011) to +1.3°C (observed on 20-January-2011) (Figure 2a), while the extreme hourly averaged temperatures were observed at -30.4°C on 5-August-2011 and +3.1°C on 31-January-2011. Temperatures are lower during the winter period as incoming solar radiation reduces to approximately zero values.

High winds are observed throughout the year (Figure 2b), with the highest daily average value recorded at 27.8 m/sec on 25-August-2011. The maximum hourly averaged wind speed observed was 38.6 m/sec on 20-June-2011. Monthly average wind speeds are higher during the winter months, and the wind direction from the high interior of the continent outward and downward towards the coast indicates that the winds are largely katabatic in origin.

Daily averaged relative humidity varies between 33% to 94% (Figure 2c), and monthly averages are fairly constant, around 50-60% throughout the year, with a yearly average of 57%. Low relative humidity was observed at the location compared to reported values at other locations on the continent. This may be because the observation site is close to Schirmacher Oasis, an exposed rocky area of approximately 19 x 3 square kilometers.

Atmospheric pressure at the observation site varies between 919 mb to 973 mb (Figure 2d) during the observation period, with a yearly average of 939 mb.

Zero sunshine hours were observed during May, June, and July, as the sun remains below the horizon during this period. From August-2011 onwards, sunshine hours start increasing as the solar elevation angle rises above the horizon. The maximum sunshine hours, 17 hours, were observed on 11-January-2011 at the observation site, after which they began to decrease from January onwards (Figure 2e).

Most days at the location were observed to be cloudy. Out of 395 observation days, only 4 days had clear sky conditions, while 43 days were overcast, and the remaining days had fractional cloud cover ranging from 1 to 7 Octa. Figure 2(f) shows the variation of daily average cloud cover in Octa (cloud type is not shown in the figure).

Fig. 1: *AWS Location near Schirmacher Oasis*

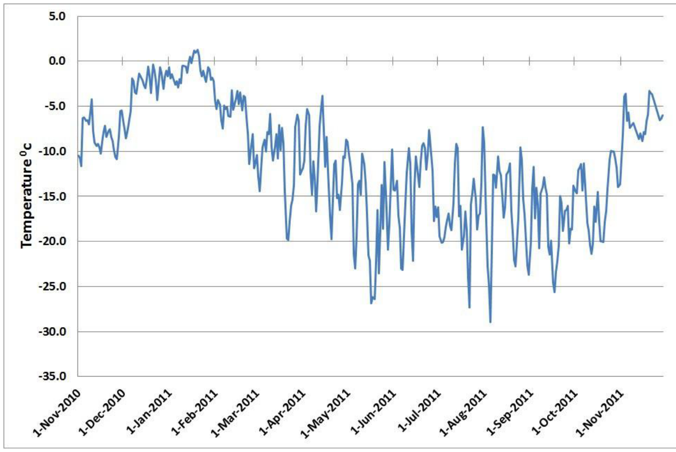

Fig. 2(a): *Daily Average Air Temperature*

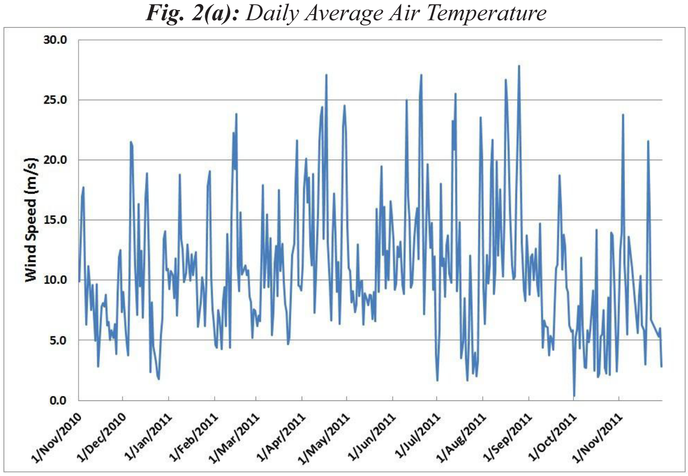

Fig. 2(b): *Daily Average Wind Speed*

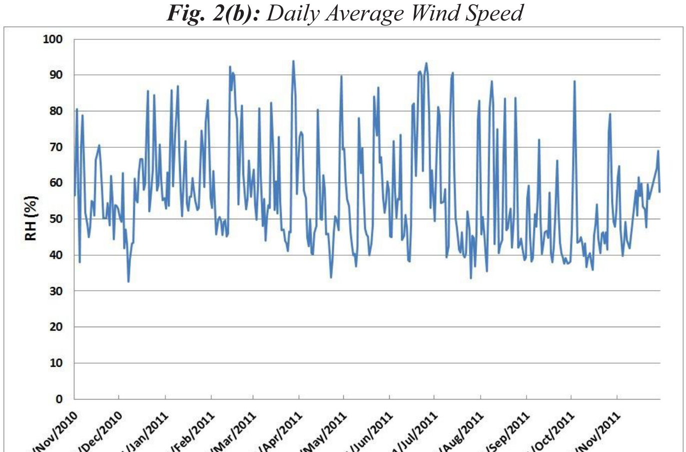

Fig. 2(c): *Daily Average Relative Humidity*

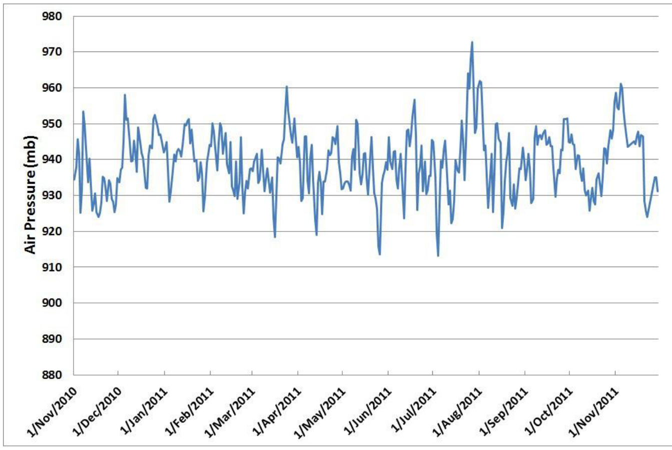

Fig. 2(d): *Daily Average Atmospheric Pressure*

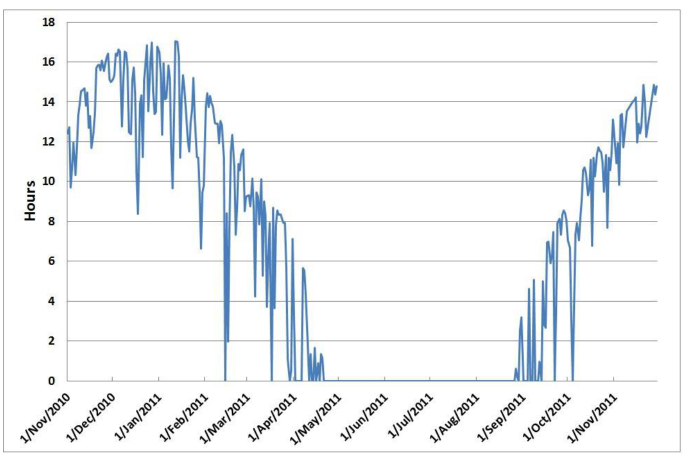

Fig. 2(e): *Daily SunShine Hours*

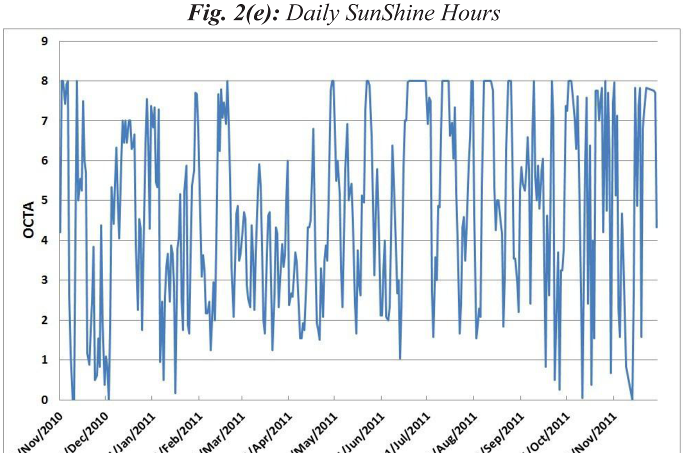

Fig. 2(f): *Daily Average Cloud Amount*

4.2 Variation of Estimated Energy Fluxes

The hourly energy budget of the ice sheet is estimated from the observed hourly meteorological parameters. The hourly values of estimated energy fluxes are summed and averaged into daily energy values. Figures 3(a), 3(b), 3(c1), 3(c2), 3(d), 3(e), 3(f), and 3(g) show the variation of daily averaged values of effective shortwave flux, effective longwave flux, longwave flux during clear sky days, longwave flux during overcast days, net radiation flux, sensible heat flux, latent heat flux, and net energy budget of the ice sheet during the observation period, respectively. The seasonal cycle of the surface energy balance based on monthly means is presented in Figure 4.

The magnitude of daily averaged effective shortwave flux varies from 2.9 W/m² to 172.7 W/m² (Figure 3a). During the peak winter months (May, June, and July), the magnitude of effective shortwave flux was observed to be almost zero, as the solar disk remains below the horizon during these months.

From August onwards, up to the end of September, the shortwave flux increased gradually, and from October onwards, a sharp increase was observed. November, December, and January are the peak summer months, during which the effective shortwave flux observed its maximum, with monthly means ranging from 0.3 W/m² to 119.4 W/m² (Figure 4). The maximum value of daily averaged effective shortwave flux was 169.4 W/m² on 30-Dec-2010. From February onwards, the shortwave flux starts decreasing, and from April onwards, it decreases sharply towards near-zero values.

During the winter months (May, June, July, and August), the net shortwave flux was almost zero. Shortwave flux was also affected by the presence of clouds, as clouds reflect some of the incident solar radiation, reducing the magnitude of downwelling radiation reaching the glacier surface.

The ice sheet is continuously ablating energy in the form of longwave radiation, and the magnitude of daily averaged effective longwave flux varies from -78.3 W/m² to -14.6 W/m² (Figure 3b). Monthly means of effective longwave flux (Figure 4) show a relatively constant cooling of the glacier, ranging from 30 W/m² to 60 W/m². During the winter period, energy ablation due to longwave flux is observed to be lower compared to the summer period. This is likely because the surface temperature of the glacier increases during summer due to absorption of significant amounts of shortwave radiation, leading to the emission of more upwelling longwave radiation.

Effective longwave flux is strongly affected by the presence of cloud cover in the atmosphere, as clouds re-emit a higher magnitude of longwave radiation to the glacier surface compared to clear air, thereby increasing the significant magnitude of downwelling longwave radiation. Figures 3(c1) and 3(c2) show the estimated daily average effective longwave flux on clear sky days (when cloud cover was 0 octa) and overcast days (when cloud cover was 8 octa) observed during the study period. The mean of the estimated effective longwave flux during clear sky days was observed to be quite high (-71 W/m^2) compared to the mean during overcast days (-29 W/m^2), indicating a very high rate of cooling of the glacier during clear sky days.

The net radiation or radiation balance is the sum of the effective shortwave and longwave components. It indicates the extent to which a surface is gaining energy through a surplus of incoming solar radiation compared with emitted terrestrial radiation or, when there is little shortwave flux, the degree to which energy is being lost from the surface. Figure 3(d) shows the temporal variation of daily averaged net radiation flux.

Net radiation flux is a major heat sink during a large part of the year and becomes a heat source for the glacier during the peak summer period. The daily averaged magnitude varies from -68.6 W/m^2 to 113.3 W/m^2. The monthly mean of the net radiation flux becomes positive for the months of October, November, December, January, and February, with the highest magnitude in December (mean value of 63.3 W/m^2).

Sensible heat flux arises as a result of temperature differences and wind activity over the glacier surface. Figure 3(e) shows the variation of estimated daily averaged sensible heat flux, which was found to be positive throughout the year at the observation site, indicating a heat source term for the glacier surface. The magnitude of the daily averaged sensible heat flux varies from 0 W/m^2 to 45.9 W/m^2 during the observation period. The monthly mean for the summer months was lower compared to other months of the year (Figure 4), as the temperature difference between the air and ice surface was observed to be low in the summer period.

When latent heat flux is positive, the saturated vapor pressure of air over the glacier surface is more than the saturated vapor pressure of the glacier surface, and water vapor condenses or deposits onto the glacier surface. Negative latent heat flux indicates the evaporation or sublimation processes over the glacier surface.

At the study location, negative latent heat flux of high magnitude was estimated throughout the observation period. For most observation days, the daily averaged latent heat flux varies from -315 W/m^2 to 0 W/m^2 (Figure 3f). The mean monthly average of latent heat flux was estimated to be -61.9 W/m^2, indicating high energy ablation from the glacier surface in the form of evaporation and sublimation.

The surface energy budget is the net flux into or out of the glacier surface. A positive surface energy budget indicates the gain of energy by the surface, while a negative budget indicates energy ablation from the glacier surface. The energy gained by the surface can be used to raise the temperature of the ice sheet or gain mass through condensation, while the energy lost can cause mass loss through phase changes (ice to water or vapor) or cooling of the glacier.

Large temporal variation was observed in the daily averaged net energy budget of the ice sheet at the study location, ranging between -477 W/m² to +3.4 W/m² (Figure 3g). The net energy budget was positive on some summer days when the magnitude of net radiation was large enough to counterbalance the magnitude of latent heat flux. Overall, the mean monthly net energy budget of the glacier was negative (Figure 4), indicating high energy ablation from the glacier surface.

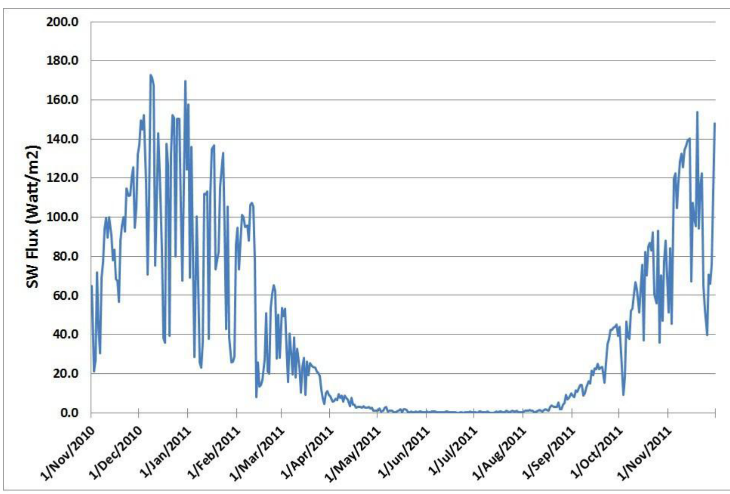

Fig. 3(a): *Variation of daily average Short Wave Flux*

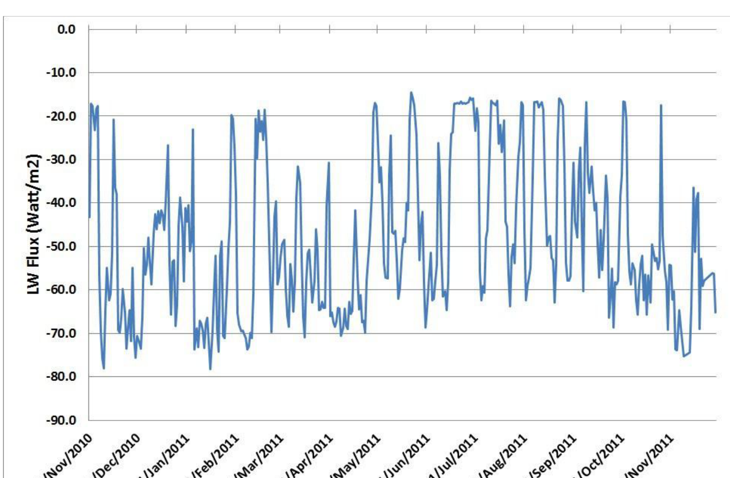

Fig. 3 (b): *Variation of daily average Long Wave Flux*

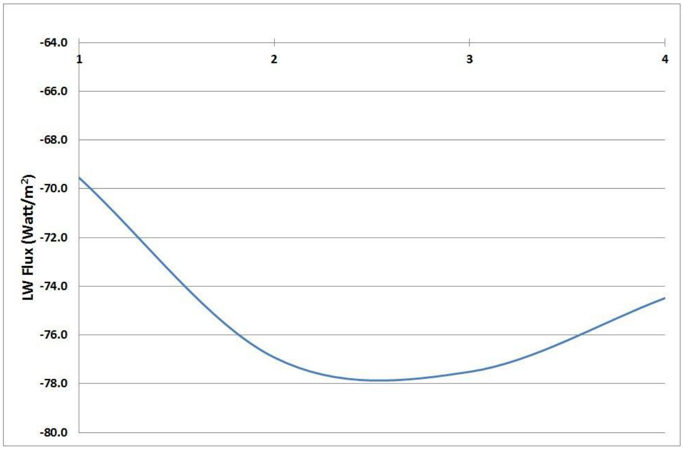

Fig. 3(c1): *Estimated Long Wave Flux on clear sky days*

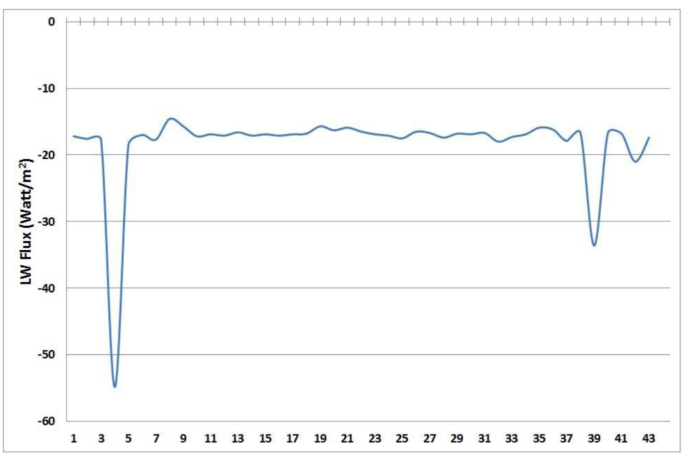

Fig. 3(c2) : *Estimated Long Wave Flux on overcast days*

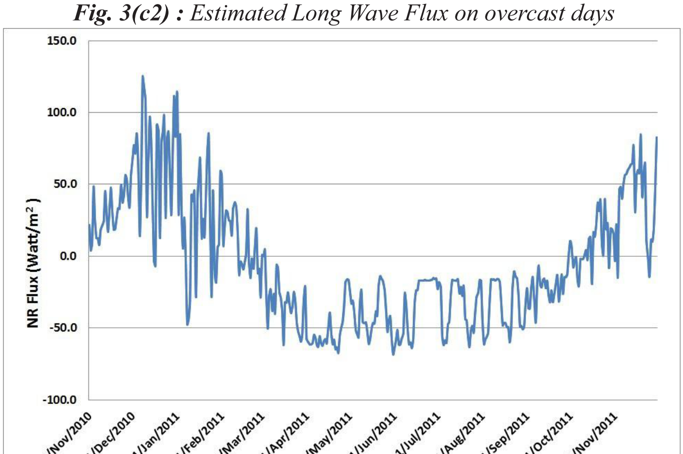

Fig. 3(d): *Variation of daily average Net Radiation Flux*

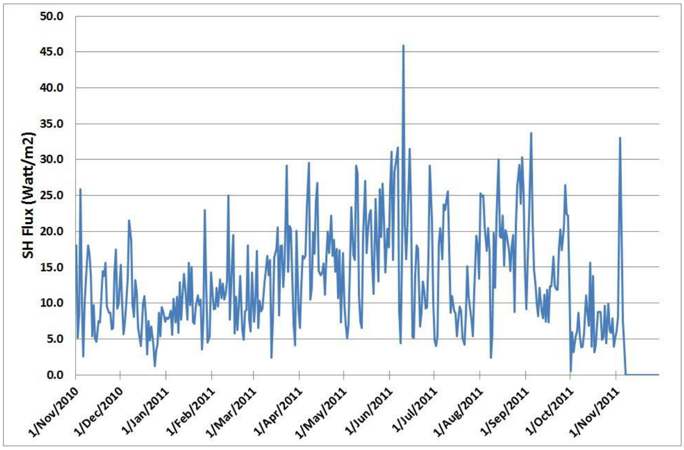

Fig. 3(e): *Variation of daily average Sensible Heat Flux*

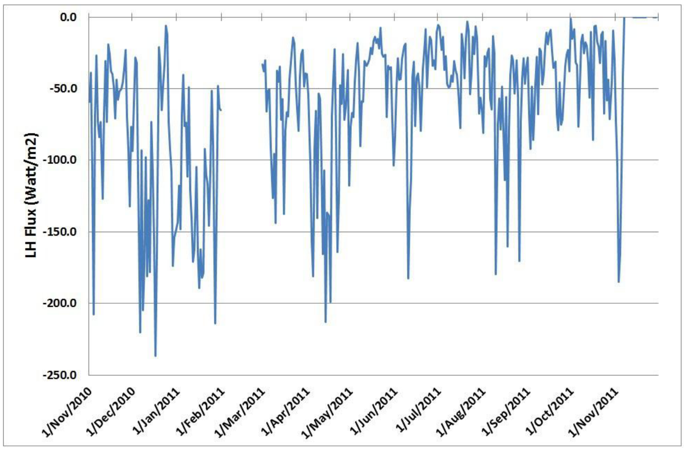

Fig. 3(f): *Variation of daily average Latent Heat Flux*

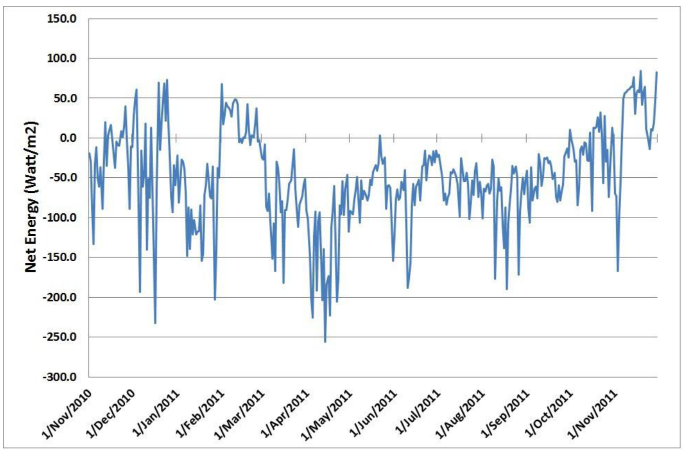

Fig. 3(g): *Variation of daily average Net Energy Balance*

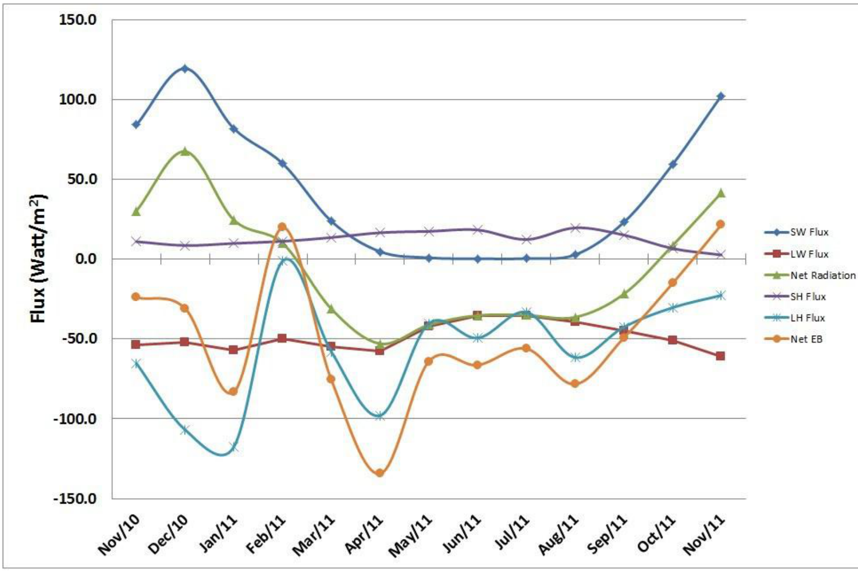

Fig. 4: *Variation of mean monthly Energy Fluxes*

Conclusions

The study was conducted during the 30th Indian Scientific Expedition to Antarctica. The results are based on observations collected from an Automatic Weather Station installed at a low-elevation, downslope location on the continental ice sheet, near the Schirmacher Oasis. The Schirmacher Oasis is an exposed rocky area of around 19 x 3 km^2 with low-lying hills. It appears that the meteorological conditions at the study site are significantly influenced by the oasis, as relative humidity values were observed to be low (yearly mean ~ 57%). Such low relative humidity values in Antarctica have also been reported earlier over blue ice surfaces located in dry valleys and near mountain ranges.

High katabatic winds were observed throughout the study period at the observation site, with a yearly mean of approximately 10.7 m/sec. The surface energy balance was evaluated using a simple model and measured hourly meteorological parameters. Effective shortwave radiation and sensible heat flux were found to be the primary heat sources for the ice sheet, while effective longwave radiation flux and latent heat flux were the main heat sinks.

In the present study, a high magnitude of effective longwave flux was estimated at the location, despite the fact that most days were cloudy. A very high magnitude of latent heat flux was also observed at the study site, with a yearly mean of -61.9 W/m^2, indicating a very high evaporation/sublimation rate of the glacier at the observation site. Low relative humidity values and high wind speeds may be the cause of this high sublimation rate, as low relative humidity and high wind speeds increase evaporation/sublimation rates from the ice surface.

Latent heat flux values of the order of -59.3 W/m² for the summer period and -40.1 W/m² for the winter period have also been reported earlier for the Dronning Maud Land area. The surface energy fluxes reported in this study on the ice sheet near the Schirmacher Oasis align with findings from earlier investigations.

Acknowledgements

The authors are grateful to the National Centre for Antarctic and Ocean Research (NCAOR), India, for providing the opportunity to participate in the Indian Scientific Expedition to Antarctica. The authors thank Sh. Ashwagosha Ganju, Director, Dr. V. D. Mishra, and Dr. H. S. Gusain for their guidance and extensive support during the study in Antarctica.

We are also thankful to the leader of the 30th Expedition, Sh. K. Jeeva, and all the members of the 30th Indian Scientific Expedition for providing logistical support and cooperation throughout the expedition period.

References

1. Acmerman, Steven A., and Knox, John A., (2003) *Meteorology—Understanding the Atmosphere*, Thomson Brooks/Cole.
2. Ambach, W., and Kirchlechner, P., (1986). Nomographs for the determination of meltwater from ice and snow surfaces by sensible and latent heat, *Wetter Leben.*, 38(4), 181–189.
3. Bintanja, R., and Van Den Broeke, M.R.(1994). Local climate, circulation and surface-energy balance of an Antarctic blue-ice area, *Annals of Glaciology*, 20, 160–168.
4. Bintanja, R. (1995). The local surface energy balance of the Ecology Glacier, King George Island, Antarctica: measurements and modelling, *Antarctic Science*, 7(3), 315–325.
5. Braithwait, Roger J., Konzelmann, Thomas, Marty, Christoph, and Olesen, Ole B. (1998), Reconnaissance study of glacier energy balance in North Greenland, 1993–94, *Journal of Glaciology*, 44(147), 239–247.
6. Braun, M., and Schneider, C. (2000), Characteristics of summer energy balance on the west coast of the Antarctic Peninsula, *Annals of Glaciology*, 31, 179–183.
7. Corps of Engineers, US Army North Pacific Division publication, *Snow Hydrology*, 1956.
8. Dozier, J., and Warren, S.G. (1982). Effect of viewing angle on the infrared brightness temperature of snow, *Water Resources Research*, 18, 1424–1434.
9. Ganju, A., Satyawali, P.K., Singh, Amreek, and Sethi, D.N.(1999). Snow cover simulation model—A review, *Defence Science Journal*, 49(5), 419–436.
10. Gruell, W., and Oerlemans, J.(1986) Sensitivity studies with a mass-balance model including temperature profile calculations inside the glacier, *Z. Gletscherkd Glazialgeol.*, 22(2), 101–124, 1986.

11. King, J.C., and Turner, J. (1997). *Antarctic Meteorology and Climatology*, Cambridge University Press.

12. Konzelmann, T., and Braithwaite, R.J.,(1995) Variations of ablation, albedo, and energy balance at the margin of the Greenland ice sheet, Kronprins Christian Land, eastern North Greenland, *Journal of Glaciology*, 41(137), 174–182.

13. Launiainen, J., and Cheng, B.(1998), Modelling of ice thermodynamics in natural water bodies, *Cold Regions Science and Technology*, 27, 153–178.

14. Mishra, V.D.,(1999). Albedo variations and surface energy balance in different snow-ice media in Antarctica, *Defence Science Journal*, 49(5), 347–362.

15. Oerlemans, J.,(1991–1992). A model for the surface balance of ice masses, Part 1, Alpine glaciers, *Z. Gletscherkd Glazialgeol.*, 27–28, 63–83.

16. Oerlemans, J., and Fotuin, J.P.F.(1992) Sensitivity of glaciers and small ice caps to greenhouse warming, *Science*, 258(5079), 115–117.

17. Paterson, W.S.B.(1994), *The Physics of Glaciers*, Third Edition, Oxford etc., Elsevier.

18. Prata, A.J.(1996). A new longwave formula for estimating downward clear-sky radiation at the surface, *Q.J.R. Meteorol. Soc.*, 122, 1127–1151.

19. Price, A.G., and Dunne, T.(1976), Energy balance computation of snowmelt in a Sub-Arctic Area, *Journal of Resource*, 12(4), 686–694.

20. Srivastava, P.K.(2002) A comparative study of glacio-meteorological parameters, reflectance, and surface energy exchange over different snow-ice media in Dronning Maud Land in East Antarctica, *Scientific Report*, Eighteenth Indian Expedition to Antarctica, Technical Publication No. 16, 153–190.

21. Upadhyay, D.S. (1995), *Cold Climate Hydrometeorology*, pp. 213–220, New Age International (P) Ltd.

22. Van De Wal, R.S.W., and Russell, A.J., (1994) A comparison of energy balance calculations, measured ablation, and meltwater runoff near Sondre Stromfjord, West Greenland, *Global and Planetary Change*, 9(1–2), 29–38.

23. Van Den Broeke, Michiel, Reijmer, Carleen, Van As, Dirk, and Boot, Wim (2006) Daily cycle of the surface energy balance in Antarctica and the influence of clouds, *International Journal of Climatology* (in press), Published online in Wiley InterScience (www.interscience.wiley.com), DOI: 10.1002/joc.1323.

24. Van Den Broeke, Michiel, Reijmer, Carleen, Van As, Dirk, Van De Wal, Roderik, and Oerlemans, J. (2005) Seasonal cycles of Antarctic surface energy balance from automatic weather stations, *Annals of Glaciology*, 41, 131–139.